

See discussions, stats, and author profiles for this publication at: <https://www.researchgate.net/publication/231394851>

Dynamic Properties of SDS Micelle Detected with "Radical-Pair-Probe" Using the Pulse-Mode Product-Yield-Detected ESR Technique

ARTICLE *in* THE JOURNAL OF PHYSICAL CHEMISTRY · APRIL 1995

Impact Factor: 2.78 · DOI: 10.1021/j100017a025

CITATIONS

11

READS

25

3 AUTHORS, INCLUDING:



Nikolay Polyakov

Institute of chemical kinetics and combustio...

85 PUBLICATIONS 778 CITATIONS

SEE PROFILE



Kazumi Toriyama

National Institute of Advanced Industrial Scie...

65 PUBLICATIONS 496 CITATIONS

SEE PROFILE

Dynamic Properties of SDS Micelle Detected with “Radical-Pair-Probe” Using the Pulse-Mode Product-Yield-Detected ESR Technique

Masaharu Okazaki,* Nikolai E. Polyakov,[†] and Kazumi Toriyama

National Industrial Research Institute of Nagoya, Hirate, Kita, Nagoya 462, Japan

Received: October 13, 1994; In Final Form: January 14, 1995[®]

The decay process of the radical pair produced in the photoreduction of anthraquinone in micellar solutions of sodium dodecyl sulfate (SDS) at various concentrations was observed by the pulse-mode product-yield-detected ESR technique. The rate of separation of the two components of the radical pair (k_{ESC}), SDS radical and anthrasemiquinone radical, decreased steeply with increasing SDS concentration, reached a minimum value at about 50 mM, and increased gradually with a further increase of concentration. The decrease in k_{ESC} in the low-concentration region has been attributed to the decrease in the rate of monomer exchange between the micelle and the bulk phase. On the other hand, the gradual increase in k_{ESC} in the high-concentration region has been assigned to the fusion/fission process of the micelle.

Introduction

The spherical micelle is a nanometer-sized molecular aggregate formed in an aqueous solution of amphiphilic molecules, such as sodium dodecyl sulfate (SDS).^{1–3} Many relaxation studies^{4–8} have been performed to clarify the details of the dynamic properties of the micelle. Two main processes are suggested:^{4–10} one is the stepwise absorption/desorption of monomers,^{6,9,10} and the other is the fusion/fission of the clusters. On the basis of only the former process, many theoretical analyses on the relaxation phenomena have been made.^{4–10} Instead of taking account of the latter explicitly, an approximation that the concentration of aggregates smaller than the proper micelle is negligible has been employed.^{4,5,7,9} However the latter process is now recognized as an important one, especially for a micellar solution at a high concentration.^{4,6,9} To break through into a new stage of understanding about the dynamical features of the micelle, observations from different viewpoints are necessary.

We have recently developed a technique, pulse-mode product-yield-detected ESR (PYESR),^{11,12} to measure the rate of escaping of the radical pair from the micelle where the radical pair is produced as the reaction intermediate of a photochemical hydrogen abstraction reaction. Since one component of the radical pair is the SDS radical,^{13,14} which should behave in an almost identical way with the intact SDS molecule, the escape process of the radical pair can be a very good probe to detect the dynamic properties of the micelle. In the present study, we have measured the lifetime of the transient radical pair composed of a SDS radical and an anthrasemiquinone radical, which are produced in the hydrogen abstraction reaction by the photochemically-excited anthraquinone molecule. The escape rate of the SDS radical from the original micelle, which can be obtained from the decay rate of the radical pair, as a function of the total SDS concentration allowed us to obtain the rates of two processes: (1) the exchange reaction of SDS monomers between the micelle and the bulk aqueous phase and (2) the fusion/fission process of micelles. Although the latter process has been clearly indicated for microspheres of the reversed micelle,^{15,16} it has been neglected for ordinary micelles, since a

large electrostatic repulsion is expected between micelles and the rate is small and difficult to detect. There are many studies on the radical-pair-decay kinetics in micelles^{17–21} made using the transient optical absorption method. However, using the optical absorption technique, it is impossible to detect the difference between the free radicals with and without the radical-pair-interaction. Therefore analysis of the decay kinetics of the radical pair in those previous reports has been made with a very simplified model.^{17–21}

Experimental Section

Sodium dodecyl sulfate (SDS) was purchased from Nakarai Chemicals (Kyoto) as the purest grade and used without further purification. Guaranteed grade anthraquinone from Wako Pure Chemicals (Tokyo) was recrystallized from ethanol. Dibromonitrosobenzenesulfonate (DBNBS) was synthesized following the literature procedure.³⁵ The concentration of anthraquinone was adjusted by monitoring the optical absorption spectrum. The temperature of the system was kept constant by using a controller (Shinko Technos MCD-130, Osaka) with N₂ gas flow. The details of the apparatus were given elsewhere.^{28,29} The well degassed SDS micellar solution containing anthraquinone and DBNBS (spin trap) was supplied to the ESR flat cell (10 × 40 × 0.25 mm³) using a flow system and was irradiated with 355 nm light from a YAG laser (Spectra Physics, GCR 150/10, 355 nm, 10 Hz, 20 mJ) and the microwave pulse (9.4 GHz, 10 W, 10 μs). The time correlation between the laser and the microwave pulses was preset using one of the two pulse sequences shown in the inset of Figure 2. The microwave power of 10 W corresponds to about 0.4 mT in the rotating frame. The conversion rate of the photoreaction was less than 35%.

Methodology and Results

The micelle can entrap hydrophobic molecules and serves as an unique reaction field for them. An interesting example is that large magnetic field effects are observed in many chemical reactions in micellar solutions.^{22–24} This phenomenon is closely related with the fact that long-lived radical pairs are produced as the intermediates in those reactions, for example, photoreduction of a quinone or a ketone in micellar solutions. We have been using the spin-trapping technique^{31,32} to study the mechanism of magnetic-field dependent photochemical

* On leave from Institute of Chemical Kinetics and Combustion, 630090 Novosibirsk, Russia.

[®] Abstract published in *Advance ACS Abstracts*, April 1, 1995.

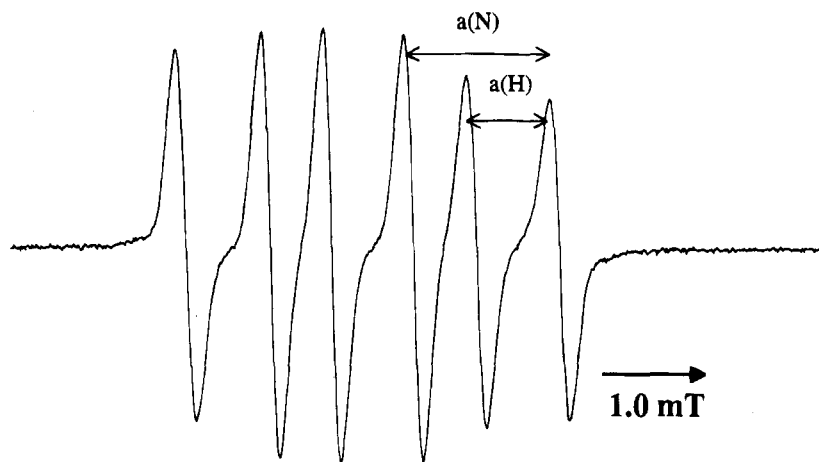
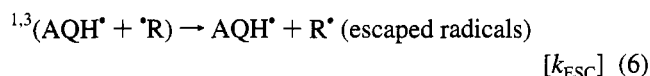
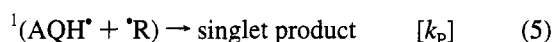
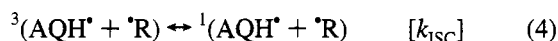
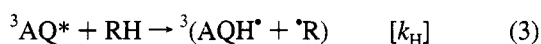


Figure 1. ESR spectrum of the spin adduct detected for the photochemical reaction of anthraquinone in SDS micellar solution. The hyperfine coupling of 1.43 mT is due to the nitrogen nucleus of the spin trap and that of 0.83 mT is due to the α -proton of the SDS radical. Therefore the SDS radical is trapped as a secondary alkyl radical. Anthrasemiquinone is not detected as the spin adduct.

reactions, since with this method one of the components of the radical pair is taken up from further reaction steps as a stable product (spin adduct) and consequently the magnetic-field effect is not deteriorated.



Where R^{\bullet} represents a free radical, $T-NO$ a spin trap, and $T-(R)NO^{\bullet}$ a spin adduct, which is a stable free radical and can be observed with the conventional ESR technique. Photoreduction of anthraquinone in an SDS micelle, used as the probe reaction here, proceeds as follows:³³



Here, AQ represents anthraquinone, which is excited by an UV photon to the singlet excited state. Intersystem crossing occurs from the lowest excited singlet state to the lowest triplet state (eq 2), which has a relatively long lifetime and thus can abstract a hydrogen atom from a hydrogen donor (RH), SDS in the present case. Consequently a radical pair constituted of anthrasemiquinone (AQH^{\bullet}) and an alkyl radical (R^{\bullet}) of SDS is formed in the triplet state (eq 3). Conversion between the singlet and the triplet states occurs due to magnetic interactions within the radical pair (eq 4). The coupling reaction proceeds only from the singlet radical pair (eq 5), but the escaping process occurs for the radical pair in both the spin states (eq 6).

Figure 1 shows the ESR spectrum of the spin adduct detected in the present system. The six-line structure comes from the hyperfine couplings with a nitrogen nucleus ($a(N)$) and a proton ($a(H)$), which were originally in the spin trap and the trapped SDS radical (α -proton), respectively. Thus semiquinone radical of anthraquinone is not trapped, probably due to a low reactivity of the spin trap to oxygen-centered radicals. The fact that only the secondary alkyl radical is formed as the intermediate from SDS was further confirmed from the shape of the product-yield-

detected ESR spectrum, where one α -proton and four β -protons were identified.²⁵

"Radical-pair probe" is a methodology in which a radical pair is used as a probe to detect the dynamics of microheterogeneous system. The principle of the method is described briefly.^{11,12} The initial spin state of the radical pair is one of the three triplet sublevels (T_0 , T_1 , T_{-1}). All of those are allowed to mix with the S state in low field, but only the T_0 state can mix with the S state at a field much higher than the hyperfine interactions (hfi).²²⁻²⁴ Therefore, at high fields radical pairs in the T_1 or T_{-1} state have a longer lifetimes and the probability to become escaped radicals, which may be finally spin-trapped, is very high. Thus at high fields the radical pair produced in the micellar solution decays in two stages: *the first stage* for T_0 finishes in a short time (<200 ns) via the $T_0 \rightarrow S \rightarrow$ cage product route, and *the second stage* for $T_{\pm 1}$ proceeds rather slowly ($1 \sim 10$ μ s). Three processes are considered for the second stage: (1) escaping of one of the component radicals from the micelle, (2) spin lattice relaxation to the T_0 or S state, from which cage product formation proceeds at a high rate, and (3) spin trapping of the SDS radical. The rate of process 1 can be obtained by subtracting the rate constants for the latter two processes (2 and 3) from the observed *second-stage* decay rate of the radical pair. The rate constant of spin trapping can be determined from the two sets of experiments at different spin trap concentrations. Spin lattice relaxation was estimated by the usual method^{11,34} with the parameters obtained experimentally.^{36,37}

When the microwave pulse resonant to one of the component radicals is applied, the $T_{\pm 1}$ state is converted into the T_0 state. Since cage product formation proceeds rapidly from the S state via the rapid T_0 -S mixing,²²⁻²⁴ spin adduct yield decreases by these ESR transitions. Figure 2 shows the decrease in spin adduct yield due to the microwave pulse as a function of τ . If a part of the radical pairs decays during the waiting time τ in pulse sequence a, the microwave pulse does not cause any reduction of spin adduct from this part. Thus we can estimate the decay rate of the radical pair with this sequence. On the other hand, if the microwave was put off before either the formation of the radical pair or the formation of the population difference between one of the $T_{\pm 1}$ and T_0 levels in the experiment using sequence b, no microwave effect is observed. Therefore, with sequence b we can obtain the information about the radical-pair formation process and/or the first-stage decay of the radical pair produced in the T_0 state. (That is, ESR transition is allowed between $T_{\pm 1}$ and T_0). The dotted lines

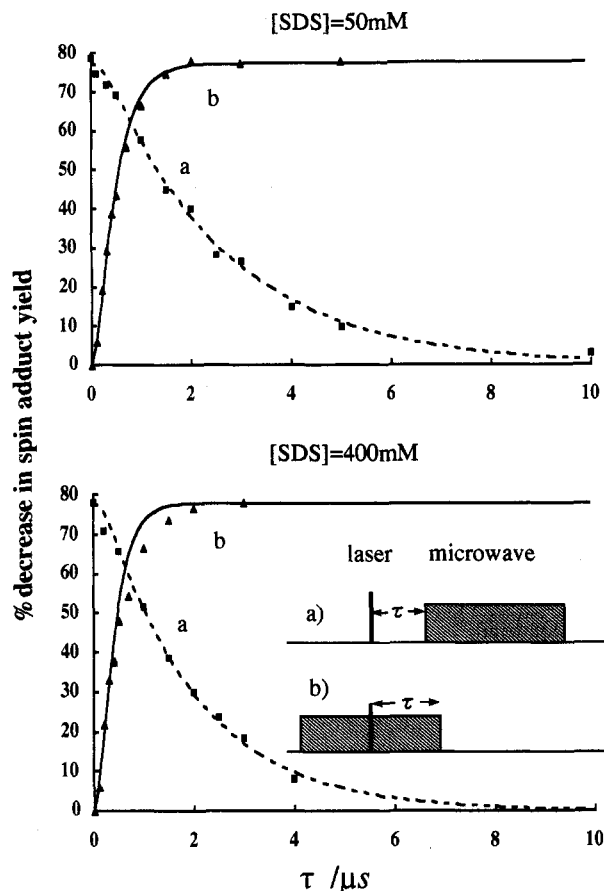


Figure 2. Response of the transient radical pair to the resonance microwave pulse as detected by the decrease in spin adduct yield at two SDS concentrations at 297 K: upper, 50 mM; lower, 400 mM. Squares and triangles are the results obtained with pulse sequences a and b, shown as the inset, respectively. Spin trap concentration was 1.0 mM. Solid and dotted lines are the calculated curves with the parameters:^{11,12} $k_H = 7.0 \times 10^6 \text{ s}^{-1}$, $k_{ISC} = 6.2 \times 10^7 \text{ s}^{-1}$, $\tau_c = 0.17 \text{ ns}$, $H_{loc} = 1.2 \text{ mT}$. Here, H_{loc} and τ_c are the local fluctuating magnetic field and its correlation time, respectively, for the spin lattice relaxation. k_{ESC} values obtained by the simulation were 1.5×10^5 and $2.3 \times 10^5 \text{ s}^{-1}$ for 50 and 400 mM, respectively.

drawn as the simulation of rectangles represent approximately the second-stage decay of the radical pair. On the other hand, the solid simulation lines for the triangles show approximately the population difference between the two groups, $(T_{+1} + T_{-1})$ and $(T_0 + S)$, as a function of τ .^{11,12,28} These simulations were made by a numerical calculation of a set of differential equations for the reaction steps in eqs 1–6 using the Runge–Kutta method.^{11,12} All the kinetic rates are obtained as the parameters in these simulations.

Figure 3 shows the escape rate of the radical pair (k_{ESC} ; closed circles) and the spin-trapping rate (k_{ST} ; closed rectangles) determined at 297 K for the photoinduced hydrogen abstraction reaction of anthraquinone in SDS micellar solution as a function of the total SDS concentration. Experiments were made with both sequences a and b (see Figure 2) for the two spin trap concentrations of 1.0 and 3.0 mM to obtain the spin-trapping rates at each SDS concentration. With increasing SDS concentration, the escape rate of the radical pair from the SDS micelle decreases initially in the low-concentration region ($\text{cmc} < C_{SDS} < 50 \text{ mM}$) but increases gradually in the high-concentration region ($50 \text{ mM} < C_{SDS} < 400 \text{ mM}$). On the other hand, the spin-trapping rate increases gradually but considerably in the low-concentration range and stays at a constant value at

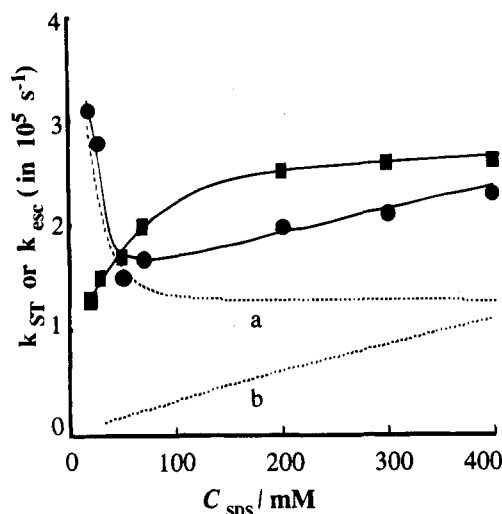
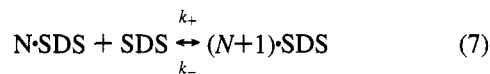


Figure 3. Escape rate (circles) and spin-trapping rate (rectangles) for the radical pair produced in the photoreduction of anthraquinone in the SDS micelle at 297 K as a function of SDS concentration. The concentration of anthraquinone was 0.06 and 0.03 mM for the systems with the SDS concentrations of ≥ 50 and $< 50 \text{ mM}$, respectively. The experimental error is less than 10% of the indicated value. The dotted lines represent the assignment of the escape rate to the two mechanisms: a for $k_{1,ESC}$ and b for $k_{2,ESC}$ (eqs 11–14).

concentrations over 0.1 M. The gradual increase in the escape rate in the high-concentration region was also confirmed at 290 K.

Discussion

According to previous studies on SDS micelle dynamics using several relaxation methods, there are two relaxation processes. One is a very rapid process which has been attributed to the exchange process of monomer surfactant between the micelle and the bulk aqueous phase (reaction 7), and the other is a slow process whose microscopic mechanism is assigned to the formation–dissolution equilibrium of the micelle (reaction 8).^{1,4–10,38} Although recent theoretical works take counterions into account explicitly,^{5,7,9,10} the simplified model below is enough for qualitative discussions.



where $N\text{-SDS}$ represents a micelle with N monomers, k_+ the rate constant of the entrapment of a monomer by the micelle, and k_- the rate constant of the release of one monomer from the micelle. k_+ for a SDS micellar solution has been estimated as $1.2 \times 10^9 \text{ M}^{-1} \text{ s}^{-1}$ at 298 K in a rather simple theoretical treatment.⁴ k_- is related with k_+ by eq 9 if the system is in equilibrium.

$$k_- = k_+[M] \quad (9)$$

where $[M]$ represents the monomer concentration. We can imagine that both k_+ and k_- are dependent very much on N , especially in the cluster region and at around the edge of the N distribution of the proper micelle. In addition, it has been pointed out that the fusion/fission process of clusters is also very important especially for the micellar solution at a high concentration.^{6,9} However, it appears very difficult to take these into account, and they have been neglected in the theoretical models.^{4,5,9} Instead of these factors, a rather intuitive ap-

proximation, that the concentration of clusters smaller than proper micelles can be neglected (narrow passage approximation), has been employed.^{4,5,9}

We can consider two processes which cause separation of the two radicals in the micelle (i.e., escape process of the radical pair). One process is due to monomer exchange (eq 7), i.e. the SDS radical included in a micelle is transferred to the bulk aqueous phase and taken up again by another micelle in a short period. The rate of this process is mainly dependent on the concentration of SDS monomer (eq 9), which is expected to decrease with an increase in the total SDS concentration due to the simultaneous increase in the counterion concentration.⁴¹ We introduce here a cross section σ_+ for the absorption of monomer by micelle, i.e.,

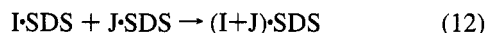
$$k_+ = k(\text{diff})' \cdot \sigma_+ \quad (10)$$

where $k(\text{diff})'$ represents the frequency of collision between the micelle and the monomer in the diffusion-limited process. Since the escape rate ($k_{1,\text{ESC}}$) of the SDS radical by the first mechanism is equal to k_-/N , we obtain eq 11 using eqs 9 and 10,

$$k_{1,\text{ESC}} = k(\text{diff})' \cdot [M] \cdot \sigma_+ / N \quad (11)$$

Here we postulate that a SDS radical behaves in exactly the same manner as an intact molecule and anthrasemiquinone is never released into the aqueous phase. It is now well-known that an increase in SDS concentration causes a decrease in monomer concentration.^{4-10,39,41} Therefore according to eq 11 a decrease in the escape rate is expected with an increase in the total SDS concentration (low-concentration region in Figure 3).

Another process should be introduced to explain the gradual increase in the escape rate in the high-concentration region of Figure 3 ($C_{\text{SDS}} > 50$ mM). A similar dependence on the total SDS concentration was found in the rate of slower relaxation phenomenon by Lessner et al.⁶ According to their study the slow relaxation rate decreases with an increase in the SDS concentration in the range less than 200 mM but the tendency is inverted in the high-concentration range (> 200 mM).⁶ They attributed the decrease in the slow relaxation rate in the low-concentration region to reaction 8 and the increase in the high-concentration range to the fusion of two SDS aggregates.^{6,9}



Although this process proceeds slowly against the electrostatic repulsion between the two clusters, the efficiency to change the micelle number should be much higher compared with that of reaction 8. We extend this model to the proper micelle as the "fusion/fission process", which should contribute to the escape process of the radical pair. The fusion/fission process has been well-characterized for the water droplet of a reversed micelle.^{15,16} We can easily imagine that when the two micelles collides, the two will fuse once but will divide into halves in a short period. In this case the radical pair collapsed at the probability of $1/2$. Thus:

$$k_{2,\text{ESC}} = k(\text{diff}) \cdot \sigma_2 \cdot (C_{\text{SDS}} - [M]) / 2N \quad (13)$$

where $k(\text{diff})$ represents the diffusion-limited rate constant ($= 8RT/3\eta$) and C_{SDS} is the total concentration of SDS molecules. σ_2 represents the cross section of effective collision for the fusion process. Since the aggregation number N changes only slightly (from 70 to 100) with an increase of SDS concentration from 50 to 400 mM (according to a small-angle neutron-scattering study⁴⁰) the concentration of micelles increases approximately linearly with C_{SDS} . Therefore, the average lifetime of the radical

pair is inversely proportional to the total SDS concentration. The observed escape rate is obtained by summing the two rates (eqs 11 and 13):

$$k_{\text{ESC}} = k_{1,\text{ESC}} + k_{2,\text{ESC}} \quad (14)$$

The dotted lines a and b in Figure 3 are the escape rates tentatively fractioned to the two mechanisms under the assumption that $k_{1,\text{ESC}}$ almost coincides with the asymptotic value at C_{SDS} 's over 100 mM. Thus the rate constant of the escaping process due to the fusion/fission process ($k_{2,\text{ESC}}$) at $C_{\text{SDS}} = 0.4$ M is estimated to be $1.1 \times 10^5 \text{ s}^{-1}$ (dotted line b). If we postulate that 100 molecules form one micelle and the diffusion limit kinetic rate constant is 2.9×10^9 ($\eta = 2.2 \times 10^{-2} \text{ P}$, $T = 297 \text{ K}$), the relative cross section σ_2 is deduced at 1.9×10^{-2} . On the other hand, the escape rate due to the monomer exchange process is about $1.3 \times 10^5 \text{ s}^{-1} \text{ M}^{-1}$ at 400 mM (dotted curve a). If we postulate that $k(\text{diff})'$ is 2.7 times as large as $k(\text{diff})$ on the basis of the ratio between the geographical cross sections of a micelle (radius is proportional to $N^{1/3}$) and a SDS monomer and that the monomer concentration is 0.6 mM,⁴¹ the relative cross section σ_1 for this process is equal to 0.86. From this simple estimation we learn that monomer exchange occurs with a high probability but fusion between the two micelles is inhibited. This small σ_2 must be due to the electrostatic repulsion between the two micelles. The cross section for the entrapment of a monomer into the micelle, σ_1 , may become rather high if the monomer approaches directing the paraffin chain to the micelle, since the hydrophobic interaction accelerates fusion and at the same time the electrostatic repulsion is suppressed to a minimum with this configuration. An increase in SDS concentration causes both a decrease in the charge of the SDS molecule, since an increase in free Na^+ is expected, and an increase of N . Since these two factors work to the opposite direction for $k_{2,\text{ESC}}$, a straight line for $k_{2,\text{ESC}}$ (line b in Figure 3) might not be a bad approximation. According to the light-scattering study,⁴¹ monomer concentrations of SDS at $C_{\text{SDS}} = 400$ mM and at $C_{\text{SDS}} = 100$ mM are about 0.6 and 1.5 mM, respectively. Therefore, the escape rate $k_{1,\text{ESC}}$ may continue to decrease even in the range $100 \text{ mM} < C_{\text{SDS}} < 400 \text{ mM}$. Taking this into account, the slope of line b may be larger than that actually drawn.

The steep increase in the spin-trapping rate with an increase of C_{SDS} ($C_{\text{SDS}} < \text{ca. } 200 \text{ mM}$) may indicate that the way of packing SDS monomers in the micelle changes with C_{SDS} . We imagine that at low concentration the negative charge of SDS may distribute on the surface of a spherical micelle, as the schematic view of the micelle we usually find in a textbook. Under this condition, the SDS radical inside the micelle is protected from the negatively charged spin trap. At high concentrations, however, due to an increase in the total Na^+ ion, the net charge of sulfate ion decreases and thus the stiffness of the micelle surface decreases. Therefore the spin trap may easily access the micelle surface to trap the SDS radical. In addition, due to a decrease in surface tension, the alkyl chain with the radical center may come out to the surface more frequently. More precise measurements are necessary for reliable partitioning of the observed escape rate into the two mechanisms of eq 13, such as the observation of the effect of additional salt.

Acknowledgment. This work was supported by a Grand-in-aid for Scientific Research on Priority Area "Molecular Magnetism" (Area No. 228/04242102) from the Ministry of Education, Science, and Culture of Japan. This work was also

supported by Special Coordination Funds for Promoting Science and Technology.

References and Notes

- (1) Langevin, D. *Annu. Rev. Phys. Chem.* **1992**, *43*, 341.
- (2) Fendler, J. H.; Fendler, E. J. *Catalysis in Micellar and Macromolecular Systems*; Academic Press: New York, 1975.
- (3) Kalyanasundaram, K. *Photochemistry in Microheterogeneous Systems*; Academic Press: Orlando, FL, 1987.
- (4) Aniansson, E. A. G.; Wall, S. N.; Almgren, M.; Hoffman, H.; Kielmann, I.; Ulbricht, W.; Zana, R.; Lang, J.; Tondre, C. *J. Phys. Chem.* **1976**, *80*, 905.
- (5) Lessner, E.; Teubner, M.; Kahlweit, M. *J. Phys. Chem.* **1981**, *85*, 1529.
- (6) Lessner, E.; Teubner, M.; Kahlweit, M. *J. Phys. Chem.* **1981**, *85*, 3167.
- (7) Elvingson, C. *J. Phys. Chem.* **1987**, *91*, 1455.
- (8) Wan-Badhi, W. A.; Palepu, R.; Bloor, D. M.; Hall, D. G.; Wyn-Jones, E. *J. Phys. Chem.* **1991**, *95*, 6642.
- (9) Wall, S.; Elvingson, C. *J. Phys. Chem.* **1985**, *89*, 2695.
- (10) Elvingson, C.; Wall, S. *J. Phys. Chem.* **1986**, *90*, 5250.
- (11) Okazaki, M.; Polyakov, N. E.; Konishi, Y.; Toriyama, K. *Appl. Magn. Reson.* **1994**, *7*, 149.
- (12) Polyakov, N. E.; Konishi, Y.; Okazaki, M.; Toriyama, K. *J. Phys. Chem.* **1994**, *98*, 10558.
- (13) Okazaki, M.; Sakata, S.; Konaka, R.; Shiga, T. *J. Am. Chem. Soc.* **1985**, *107*, 7214.
- (14) Okazaki, M.; Shiga, T. *Nature* **1986**, *323*, 240.
- (15) Jada, A.; Lang, J.; Zana, R. *J. Phys. Chem.* **1989**, *93*, 10.
- (16) Maria-Jones, S.; Levy, H.; Lang, J. *J. Phys. Chem.* **1993**, *97*, 9808.
- (17) Levin, P. P.; Kuzmin, V. A. *Chem. Phys.* **1992**, *162*, 79.
- (18) Evans, C. H.; Scaiano, J. C.; Ingold, K. U. *J. Am. Chem. Soc.* **1992**, *114*, 140.
- (19) Tanimoto, Y.; Fujiwara, Y.; Takamatsu, S.; Kita, A.; Itoh, M.; Okazaki, M. *J. Phys. Chem.* **1992**, *96*, 9844.
- (20) Khudyakov, I. V.; McGarry, P. F.; Turro, N. J. *J. Phys. Chem.* **1993**, *97*, 13234.
- (21) Wakasa, M.; Hayashi, H. *Chem. Phys. Lett.* **1994**, *229*, 122.
- (22) Turro, N. J. *Proc. Natl. Acad. Sci. U.S.A.* **1983**, *80*, 609.
- (23) Hayashi, H. In *Photochemistry and Photophysics*; Rabek, J. F., Ed.; CRC Press: Boca Raton, FL, 1990; Vol. 1, pp 59–136.
- (24) Steiner, U. E.; Wolff, H.-J. In *Photochemistry and Photophysics*; Rabek, J. F., Ed.; CRC Press: Boca Raton, FL, 1991; Vol. 4, pp 1–130.
- (25) Okazaki, M.; Sakata, S.; Konaka, R.; Shiga, T. *J. Chem. Phys.* **1987**, *86*, 6792.
- (26) Okazaki, M.; Shiga, T.; Sakata, S.; Konaka, R.; Toriyama, K. *J. Phys. Chem.* **1988**, *92*, 1402.
- (27) Tarasov, V. F.; Bagryanskaya, E. G.; Grishin, Y. A.; Sagdeev, R. Z.; Buchachenko, A. L. *Mendeleev Commun.* **1991**, 85.
- (28) Okazaki, M.; Toriyama, K. *Bull. Chem. Soc. Jpn.* **1993**, *66*, 1892.
- (29) Okazaki, M.; Konishi, Y.; Toriyama, K. *Chem. Lett.* **1994**, 737.
- (30) Okazaki, M.; Toriyama, K. *J. Phys. Chem.* **1995**, *99*, 489.
- (31) Janzen, E. G. *Acc. Chem. Res.* **1971**, *4*, 31.
- (32) Buettner, G. R. *Free Radical Biol. Med.* **1987**, *3*, 259.
- (33) Tanimoto, Y.; Udagawa, H.; Itoh, M. *J. Phys. Chem.* **1983**, *87*, 724.
- (34) Carrington, A.; McLauchlan, A. D. *Introduction of Magnetic Resonance*; Harper & Row: New York, 1967; Chapter 11.
- (35) Kaur, H.; Leung, K. W. H.; Perkins, M. J. *J. Chem. Soc., Chem. Commun.* **1981**, 142.
- (36) Baglioni, P.; Rivara-Minten, E.; Dei, L.; Ferroni, E. *J. Phys. Chem.* **1990**, *94*, 8218.
- (37) Tanimoto, Y.; Fujiwara, Y.; Takamatsu, S.; Kita, A.; Itoh, M.; Okazaki, M. *J. Phys. Chem.* **1992**, *96*, 9844.
- (38) Lang, J.; Tondre, C.; Zana, R.; Bauer, R.; Hoffmann, H.; Ulbricht, W. *J. Phys. Chem.* **1975**, *79*, 276.
- (39) Mysels, K. J.; Princen, L. H. *J. Phys. Chem.* **1959**, *63*, 1699.
- (40) Berr, S. S.; Coleman, M. J.; Jones, R. R. M. *J. Phys. Chem.* **1986**, *90*, 6492.
- (41) Corti, M.; Degiorgio, V. *J. Phys. Chem.* **1981**, *85*, 711.

JP9427544